Edge Distributed Autonomous Control Of Massive AC/DC Renewable Energy Cluster

Junni Su[1], Fengchao Chen[1], Xin Zhang[1], Lide Zhou[1], Yipeng He[1], and Hua Zheng[2*]

[1] Dongguan Power Supply Bureau of Guangdong Power Grid Co., Ltd
[2] School of Electrical and Electronic Engineering, North China Electric Power University, Beijing 102208, China
[*] Corresponding author. E-mail: hbdl_zhenghua@263.net

Received: Nov. 29, 2022; Accepted: Apr. 15, 2023

Microgrid and distributed generation are more and more widely used in power systems. In this background, a control strategy based on consistency is proposed in this paper, to improve the optimal regulation ability of the AC/DC hybrid microgrid groups. The control strategy is divided into two levels: control strategy within a subnet and control between microgrid groups. At the level of subnet control, the power mapping factor and secondary adjustment term are introduced into the traditional droop control, to realize the autonomous and stable optimization in the island mode of a single sub microgrid. At the level of inter microgrid groups control strategy, the local control strategy of interlinking converter based on average power mapping factor is constructed, and the compensation term based on consistency is introduced to realize the power optimization operation between different microgrids jointly. Finally, the simulation model is established by Matlab/Simulink to prove the effectiveness of the method.

Keywords: AC/DC hybrid microgrid groups, Power mapping factor, Distributed control, Optimized control

http://dx.doi.org/10.6180/jase.202403_27(3).0013

1. Introduction

Recent years, distributed generation (DG), represented by photovoltaic and wind turbine, has developed rapidly [1], which not only makes the distribution network more green and environmentally friendly, but also brings severe challenges to the safe and stable operation of the distribution network [2]. Microgrid, as an effective means to accept distributed generation [3], has become an important way for grid connected consumption of distributed generation [4]. However, a single microgrid has some shortcomings, such as limited working capacity and weak anti-interference ability [5], which can only meet the access requirements of local distributed power sources. Therefore, it is an important direction for the future development of microgrids to interconnect multiple heterogeneous AC and DC microgrids in close proximity [6] to form an AC/DC hybrid microgrid group [7].

The existing AC, DC and hybrid microgrids usually adopt droop control strategy to achieve balanced power distribution according to the capacity of each DG unit [8]. Although this control method can meet the autonomous operation requirements of the microgrid, it fails to consider the economic characteristics of DG units when power distribution, which can not realize the economic control of the microgrid and meet the economic operation requirements of the AC/DC hybrid microgrid group. Therefore, it is urgent to study the economic control method for AC/DC hybrid micro electric network group.

The economic control strategy of the AC/DC hybrid micro grid group can be discussed in two parts: one is the internal control strategy of the AC/DC micro grid, which is used to achieve the autonomous stability and economic power distribution within each sub micro grid; The second is the inter group control strategy of the hybrid microgrid, which is used to realize the cooperative and optimal

operation between the AC and DC subnetworks and the interlinking converter (ILC).

At present, many scholars have studied the stability control of microgrids. Reference [9] proposes a distributed quadratic control method based on the PI consistency algorithm, which is used to eliminate the estimation error generated by the voltage observer in the presence of input disturbances. And finally the control method realize the recovery of voltage/frequency and the accurate distribution of reactive/active power. Reference [10] divides the existing quadratic controllers into four categories. Based on delay margin, four types of controllers are compared, and the sensitivity expression of delay margin to system parameters in steady-state operation is further deduced theoretically. Reference [11] proposes a microgrid fully distributed power dispatching method, which can realize fast frequency recovery and minimize generation costs. In the first stage, the consistency algorithm based on a subgradient is used to recover the frequency. Reference [12] proposes a new random consistent quadratic voltage and frequency recovery method considering communication delay and derives the proof of mean-square consistent recovery using strict Lyapunov analysis. To solve the problems of distributed economic dispatching and stability optimization, reference [13] proposes a new distributed power system control scheme based on consistency. Based on considering the problems of communication noise and fault, PI frequency controller and neural network frequency controller are adopted to improve the robustness of the control method. Based on the traditional secondary voltage control method, the reference [14] establishes the nonsingular terminal sliding mode control model by introducing the error function. At the same time, the distributed controller can adjust the voltage amplitude to the reference value without considering the dynamic uncertainty and bounded external interference.

In [15], aiming at the problem of voltage and frequency recovery of isolated island microgrid, a secondary voltage and frequency recovery method based on consistency fault tolerance considering disturbance and controller fault is proposed. Reference [16] proposes a new interconnection converter called an energy networking unit (ENU). The ENU is used to connect AC and DC sub grids in a single hybrid micro grid, and also facilitates connection to external grids. Then, a hybrid microgrid cluster architecture based on ENU is established, which is scalable, reconfigurable, and modular. Thanks to the reconfigurable topology of ENU, this architecture can achieve flexible AC/DC interconnection between microgrids with fewer power conversion units and the same converter module. The vehicle-to-grid (V2G) technology is an effective and economic solution to enable the integration of electric vehicles (EVs) into power grids. As an effort to present the state of the art in relevant fields, the power interaction mode between EVs and power grids, and the scheduling methodology for the V2G implementation are overviewed comprehensively in [17]. An integrated and reconfigurable hybrid AC/DC microgrid architecture with its hierarchical control strategy is proposed in [18]. The dedicated interfaces and cluster controllers for electric vehicles (EVs) facilitate the implementation of centralized vehicle-to-grid (V2G) service. In [19], the peak shaving capacity of a user-oriented V2G scheme with multiple operation modes is surveyed compared to the conventional charging mode. The city of Shenzhen, China, is taken as a case study to evaluate the power demand of EV charging during peak hours for different scenarios. In order to obtain the coordinated EV charging strategy, the global/divided scheduling optimization model is developed for the centralized/decentralized V2G strategy.

However, only reference [13] in the above literature deals with some economic optimization problems. The research contents of other literature are all focused on the two-layer control to realize the stable recovery of voltage and frequency. At present, many scholars have focused on the three-layer control method, including economic optimization. For example, reference [20] combines the third-layer control with a consistency algorithm to minimize the total operation cost of the power grid to achieve the purpose of optimal economic dispatching. Although this three-layer control method can achieve the economic optimal dispatching goal of the power grid, its response speed is slow. In some cases, it can even reach the minute level, which will cause the mismatch between the third layer control and the traditional second layer control structure, resulting in the deviation of the actual operation of the microgrid from the optimal state, so that the optimal economic operation can not be realized.

In terms of intergroup control of hybrid microgrid, reference [21] introduces the discrete consistency control principle into the control layer of AC and DC sub microgrid to realize the accurate distribution of reactive power and DC DG current. Reference [22] proposes a distributed control method of the interlinking converter, which enables the AC and DC sub microgrid to distribute its active power according to the incremental cost and realizes the economic control of the hybrid microgrid. However, the research objects of the above literature are single hybrid microgrids, and the effectiveness of its control strategy in hybrid microgrid groups remains to be verified. To solve the prob-

lem of power distribution, optimization, and stability of AC/DC hybrid microgrid groups, reference [23] proposed a distributed collaborative control method for AC/DC hybrid microgrid groups based on event trigger mechanism, which realizes the reasonable distribution of power among different sub micro-networks through the communication interaction between interlinking converters. However, this control method does not study the optimal control method of the AC/DC hybrid microgrid groups and can not realize the economic operation of the hybrid microgrid groups.

To study the distributed autonomous economic control strategy of the AC/DC hybrid microgrid groups, this paper makes innovation from two aspects. In the element of control in a microgrid, an improved two-layer control strategy is proposed in this paper. The third layer of traditional economic optimization control is raised to the second layer, and the primary control of the first layer is improved to frequency/power mapping factor droop control to adapt to the new structure. A consistency algorithm is proposed for the second layer control. In the aspect of inter-group control, the local control strategy of the interconnected converter and the secondary control strategy based on consistency algorithm are constructed. Compared with the traditional AC/DC hybrid microgrid groups control strategy, the advantages of the control strategy proposed in this paper are as follows.

- The concept of power mapping factor is introduced into the droop control strategy, which can achieve the objectives of frequency stability and power optimization under the primary control, eliminate the action time of the third layer control, and significantly improve the optimal operational efficiency in the microgrid.
- Currently, the research on control strategies is mainly focused on the field of single AC/DC hybrid microgrid. Its structure is mainly a single communication between a single AC network and a single DC network, and its structure is relatively simple and cannot control the AC/DC hybrid microgrid group. The AC/DC hybrid micro electrical network group control strategy proposed in this paper fills the research gap in this field.

The rest of this paper is organized as follows. In Section II, the system structure and distributed control principle of the AC/DC hybrid microgrid groups are introduced. In Section III, the hierarchical distributed control strategy of the AC/DC hybrid microgrid is designed. In Section IV, an example of the system is given. Finally, Section V concludes the paper.

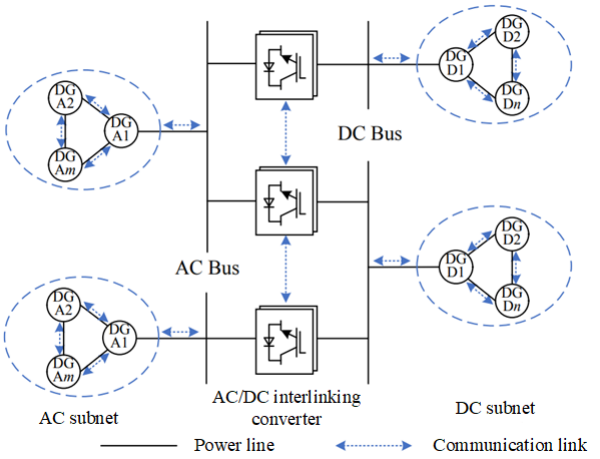

Fig. 1. AC/DC hybrid microgrid groups structure

2. System structure and distributed control principle of ac/dc hybrid microgrid groups

The structure of the AC/DC hybrid microgrid groups is shown in Fig. 1. It is composed of AC/DC subnet and ILC. Each subnet contains DG and load units. Each DG unit can communicate with neighbor nodes, and some DG units can communicate directly with ILC. From the perspective of a large power grid, there is an information path between adjacent ILCs, so that there is at least one directed information path between any two DG units in the whole network, which provides a communication network basis for the intergroup and intragroup hierarchical distributed control of AC/DC hybrid microgrid groups.

3. Distributed control strategy of ac/dc hybrid microgrid

3.1. Control objectives of AC/DC hybrid microgrid groups

3.1.1. Control objectives of AC subnet

Enable each DG in the AC subnet to distribute the active power according to the principle of equal incremental to realize the economic control of active power[24],

$$\begin{cases} \lambda_{m1} = \cdots = \lambda_{mi} = \cdots = \lambda_{mp} \\ \lambda_{mi} = 2\alpha_{mi}P_i + \beta_{mi} \end{cases}, \forall m \in N^{ac} \quad (1)$$

where λ_{mi} is the power mapping factor of the i th DG in the m th AC subnet. α_{mi} and β_{mi} is the power mapping factor coefficient. N^{ac} is the collection of AC subnet.

Restore the frequency of the AC subnet to the reference frequency,

$$\lim_{t\to\infty}(\omega_{mi} - \omega^*) = 0, \forall m \in N^{ac} \quad (2)$$

$$\lim_{t\to\infty}\left(U_{\mathrm{PCC},m}-U^{*}_{\mathrm{PCC},m}\right)=0,\forall m\in N^{ac} \tag{3}$$

Where $U_{\mathrm{PCC},m}$ and $U^{*}_{\mathrm{PCC},m}$ are the voltage measurement value and the reference value of the m th AC subnet common connection bus respectively.

Enable each DG in the AC subnet to distribute reactive power according to the principle of equal proportion distribution,

$$k^{Q}_{ac,m1}Q_{m1}=k^{Q}_{ac,m2}Q_{m2}=\cdots=k^{Q}_{ac,mp}Q_{mp},\quad \forall m\in N^{ac} \tag{4}$$

Where $k^{Q}_{ac,mi}$ and Q_{mi} are the reactive power/voltage droop coefficient and reactive power of the i th DG in the m th AC subnet, respectively. To simplify the analysis, this paper sets k^{Q}_{ac} of each DG to the same value, that is, to realize the equal distribution of reactive power among DG.

3.1.2. Control objectives of DC subnet

Enable each DG in the DC subnet to distribute active power according to the principle of equal incremental,

$$\lambda_{n1}=\cdots=\lambda_{nj}=\cdots=\lambda_{nq},\forall n\in N^{dc} \tag{5}$$

Where λ_{nj} is the power mapping factor of the j th DG in the nth DC subnet, N^{dc} is the DC subnet set.

Restore the voltage at the common bus of the DC subnet to the reference value,

$$\lim_{t\to\infty}\left(U_{\mathrm{PCC},n}-U^{*}_{\mathrm{PCC},n}\right)=0,\forall n\in N^{dc}v \tag{6}$$

Where $U_{\mathrm{PCC},n}$ and $U^{*}_{\mathrm{PCC},n}$ are the voltage measurement value and the reference value of the common connection bus of the nth DC subnet, respectively.

3.1.3. Control objectives between subnets

By controlling the transmission power of ILC, the power mapping factors of different subnets are consistent,

$$\overline{\lambda^{ac}_{1}}=\cdots=\overline{\lambda^{ac}_{m}}=\overline{\lambda^{cc}_{1}}=\cdots=\overline{\lambda^{cc}_{n}} \tag{7}$$

Where $\overline{\lambda^{ac}_{m}}$ is the mean value of the power mapping factor of the m th AC subnet, $\overline{\lambda^{dc}_{n}}$ is the mean value of the power mapping factor of the nth DC subnet.

3.2. AC subnet control strategy

The traditional primary control usually adopts $P-\omega$ droop control strategy to realize the stable operation of the system,

$$\omega_{mi}=\omega^{*}-k^{P}_{ac}P_{mi} \tag{8}$$

Where k^{P}_{ac} is droop coefficient.

The secondary control obtains the globally consistent compensation amount through the consistency algorithm for droop compensation and realizes the control goal of no difference in frequency by translating the droop characteristic curve upward. Different from the traditional control strategy, the control strategy in this paper puts the power optimization in the second layer. That is, the dual objectives of frequency recovery and power optimization are taken into account in the secondary control, which simplifies the control steps. In addition, the load in the system is unknown, so it is usually difficult to calculate the optimized active power reference value in the off-line state. If the primary control method still adopts the traditional $P-\omega$ droop control, it will significantly improve the design difficulty of the secondary control. Therefore, to better adapt to the improved secondary control strategy, the concept of power mapping factor is introduced into the primary control. Unlike the traditional droop control, this paper directly adopts droop control with an equal incremental principle. The secondary control realizes the secondary adjustment of microgrid frequency, voltage, and reactive power through the information interaction between DGs. It avoids the problems of active power distribution imbalance and system instability caused by frequency instability.

So, the corresponding DG control strategy of the AC subnet is formulated as

$$\begin{cases}\omega_{mi}=\omega^{*}-k^{P}_{ac}\lambda_{mi}+\gamma_{mi}\\ U_{mi}=U^{*}_{m}-k^{Q}_{ac}Q_{mi}+\delta_{mi}\end{cases} \tag{9}$$

Where ω^{*} and U^{*}_{m} are the frequency reference value and rated voltage of AC subnet respectively, γ_{mi} and δ_{mi} are the secondary control items of DG active and reactive power control links respectively, and k^{P}_{ac} is the power mapping factor/frequency droop coefficient of AC subnet.

The secondary control items of the DG active power control link correspond to Eqs. (1) and (2) in the control objectives of the AC subnet, including cost secondary control item γ^{λ}_{mi} and frequency secondary control item γ^{ω}_{mi} for DG active power output,

$$\gamma_{mi}=\gamma^{\lambda}_{mi}+\gamma^{\omega}_{mi} \tag{10}$$

According to the consistency principle, the power mapping factor quadratic control term to realize the economic distribution of active power is formulated as,

$$\begin{cases}\gamma^{\lambda}_{mi}=\left[\lambda^{*}_{mi}(t)-\lambda_{mi}\right]\left(k^{ac,\lambda}_{p}+\frac{k^{ac,\lambda}_{i}}{s}\right)\\ \lambda^{*}_{mi}(t)=\lambda_{mi}(t)+\sum_{j\in N_m}a_{ij}\left[\lambda_{mj}(t)-\lambda_{mi}(t)\right]\end{cases} \tag{11}$$

Where $\lambda_{mi}(t)$ and $\lambda^{*}_{mi}(t)$ are the power mapping factor of DG i at time t and the reference value updated by the consistency protocol, respectively, $k^{ac,\lambda}_{p}$ and $k^{ac,\lambda}_{i}$ are the

proportional and integral parameters of PI control, respectively.

To meet the frequency control goal of the AC subnet, the frequency secondary control item of the leading node is constructed and is formulated as

$$\begin{cases} \gamma_{mi}^{\omega} = \left[\omega_{mi}^{*}(t) - \omega_{mi}\right]\left(k_p^{\omega} + \frac{k_i^{\omega}}{s}\right) \\ \omega_{mi}^{*}(t) = \omega_{mi}(t) \\ +\sum_{j\in N_m} a_{ij}\left[\omega_{mj}(t) - \omega_{mi}(t)\right] + g_i\left[\omega_m^{*} - \omega_{mi}(t)\right] \end{cases} \tag{12}$$

Where $\omega_{mi}(t)$ and $\omega_{mi}^{*}(t)$ are the frequency value at DG i at time t and the reference value obtained from the consistency protocol including the leader node, respectively.

In terms of reactive power control, to achieve Eqs. (3) and (4) in the control goal of the AC subnet, the reactive power secondary control item can be divided into voltage control item δ_{mi}^{U} and reactive power distribution secondary control item δ_{mi}^{Q},

$$\delta_{mi} = \delta_{mi}^{U} + \delta_{mi}^{Q} \tag{13}$$

The voltage secondary adjustment component is formulated as

$$\begin{cases} \delta_{mi}^{U} = \left[U_{mi}^{*}(t) - U_{mi}\right]\left(k_p^{ac,U} + \frac{k_i^{cc,U}}{s}\right) \\ U_{mi}^{*}(t) = U_{mi}(t) + \sum_{j\in N_m} a_{ij}\left[U_{mj}(t) - U_{mi}(t)\right] \\ +g_i\left[U_{PCC,m}^{*} - U_{PCC,m}(t)\right] \end{cases} \tag{14}$$

Where $U_{mi}(t)$ and $U_{mi}^{*}(t)$ are the voltage value at DG i at time t and the reference value obtained from the consistency protocol including the leading node, respectively. g_i is the link weight between node i and the common connection bus. If node i has a communication link with ILC, it is $g_i = 1$, otherwise, it is 0.

To achieve the control goal of reactive power, the secondary control item of reactive power distribution is formulated as

$$\begin{cases} \delta_{mi}^{Q} = \left[Q_{mi}^{*}(t) - Q_{mi}\right]\left(k_p^{Q} + \frac{k_i^{Q}}{s}\right) \\ Q_{mi}^{*}(t) = Q_{mi}(t) + \sum_{j\in N_m} a_{ij}\left[Q_{mj}(t) - Q_{mi}(t)\right] \end{cases} \tag{15}$$

Where $Q_{mi}(t)$ and $Q_{mi}^{*}(t)$ are respectively the reactive power value of DG i at time t and the reference value updated by the consistency protocol.

3.3. DC subnet control strategy

Like the control strategy of the AC subnet, its control structure can also be divided into two layers. The primary control adopts the voltage droop control strategy based on the voltage/power mapping factor, which is used for the economic distribution of DC DG power. Based on the principle of consistency, the secondary control realizes the secondary adjustment of DC subnet voltage. It avoids the problem that the active output cannot be allocated according to the power mapping factor due to the unbalanced node voltage. The control strategy is formulated as

$$U_{ni} = U_n^{*} - k_{dc}^{P}\lambda_{ni} + \eta_{ni} \tag{16}$$

Where U_n^{*} is the rated voltage of DC subnet, η_{ni} is the secondary control item of DG active power, and k_{dc}^{P} is the power mapping factor/voltage droop coefficient of DC subnet.

According to Eqs. (9) and (10) in the control objectives, it is also composed of cost adjustment component η_{ni}^{U} and DC voltage adjustment component η_{ni}^{λ} of DG active output,

$$\eta_{ni} = \eta_{ni}^{U} + \eta_{ni}^{\lambda} \tag{17}$$

Similarly, we can construct the secondary control item of DC subnet DG cost according to Eq. (15),

$$\begin{cases} \eta_{ni}^{\lambda} = \left[\lambda_{ni}^{*}(t) - \lambda_{ni}\right]\left(k_p^{dc,\lambda} + \frac{k_i^{dc,\lambda}}{s}\right) \\ \lambda_{ni}^{*}(t) = \lambda_{ni}(t) + \sum_{j\in N_n} a_{ij}\left[\lambda_{nj}(t) - \lambda_{ni}(t)\right] \end{cases} \tag{18}$$

In terms of DC voltage control, it is also necessary to consider the convergence of node voltage to the mean value and the tracking of reference value by common connection bus. Therefore, the corresponding voltage secondary control item is formulated as

$$\begin{cases} \eta_{ni}^{U} = \left[U_{ni}^{*}(t) - U_{ni}\right]\left(k_p^{dc,U} + \frac{k_i^{dc,U}}{s}\right) \\ U_{ni}^{*}(t) = U_{ni}(t) + \sum_{j\in N_n} a_{ij}\left[U_{nj}(t) - U_{ni}(t)\right] \\ +g_i\left[U_{PCC,n}^{*} - U_{PCC,n}(t)\right] \end{cases} \tag{19}$$

Where $U_{ni}(t)$ and $U_{ni}^{*}(t)$ are the voltage value at DG i at time t and the reference value, respectively.

3.4. Control strategy between subgroups of microgrid

The AC and DC sub microgrids are connected through ILC. ILC realizes the independent balance of each sub microgrid by controlling the exchange of power between each sub microgrid and maintains the stability of the AC and DC hybrid microgrid. To simplify the analysis, this paper sets ILC to operate at unity power factor. That is, it only undertakes the tasks of active power transmission between microgrids, frequency recovery of AC subnet and voltage recovery of DC subnet. Finally, the control objective Eq. (7) is realized by controlling each ILC.

The control objective Eq. (7) can be analyzed from two aspects: one is to make the average power mapping factor of the AC subnet and DC subnet directly connected to ILC the same, which is formulated as

$$\begin{cases} f_g = \overline{\lambda_n^{dc}} - \overline{\lambda_{mn}^{ac}} \\ \lim_{t\to\infty} f_g = 0 \\ \overline{\lambda_m^{ac}} = \sum_{i\in N_m} g_i \cdot \lambda_{mi} \\ \overline{\lambda_n^{dc}} = \sum_{i\in N_n} g_i \cdot \lambda_{ni} \end{cases} \tag{20}$$

Where $\overline{\lambda_m^{ac}}$ is the average power mapping factor of the m AC subnet connected to the interlinking converter ILCg, and $\overline{\lambda_n^{dc}}$ is the average power mapping factor of nth DC subnet connected to ILCg. f_g is the difference in the average power mapping factor between the two subnets. The calculation method of the average power mapping factor of each subnet is as follows. The DG communicating with ILC in each subnet transmits the power mapping factor at the current sampling time to the converter station and calculates the average value.

So, the ILC active power control strategy is constructed in the positive direction of injecting power from the AC power grid to the DC power grid,

$$P_{ILC,g}^{*} = f_g \left(k_p^{\mathrm{ILCC}} + \frac{k_i^{\mathrm{ILCC}}}{s} \right) \tag{21}$$

where $P_{IC,g}^{*}$ is the setting value of ILC transmission power.

In addition, as an active power transmission device, ILC can also participate in the frequency control of AC microgrid and the voltage control of DC microgrid public connection bus to speed up the stable recovery process of sub microgrid. Therefore, the auxiliary control is formulated as

$$\begin{cases} \gamma_g^{\omega} = \left(k_p + \frac{k_i}{s} \right) \left(\omega_{\mathrm{pu}}^{*} - \omega_{\mathrm{pu}} \right) \\ \eta_g^{U} = \left(k_p + \frac{k_i}{s} \right) \left(U_{\mathrm{PCC,pu}}^{*} - U_{\mathrm{PCC,pu}} \right) \end{cases} \tag{22}$$

Where ω_{pu}^{*} and ω_{pu} are the normalized values of the reference frequency and the actual measured frequency of the common connection bus on the AC side, respectively. $U_{\mathrm{PCC,pu}}^{*}$ and $U_{\mathrm{PCC,pu}}$ are the normalized values of the reference voltage and the actual measured voltage of the DC side common connection bus, respectively.

So, the corresponding ILC primary control strategy is formulated as

$$P_{IC,g}^{*} = f_g \left(k_p^{\mathrm{ILCC}} + \frac{k_i^{\mathrm{ILCC}}}{s} \right) - \gamma_g^{\omega} + \eta_g^{U} \tag{23}$$

where γ_g^{ω} and η_g^{U} are obtained according to the local measurement information of ILC.

f_g is obtained from the power mapping factor information of ILC local subnet. However, the primary control strategy of ILC only considers the power mapping factor of the bilateral subnet directly connected by the local ILC, which is easy to lead to the power snatching of the same subnet between each ILC. For the sub microgrid with relatively small capacity, a slight change in switching power will have a significant impact on the power mapping factor of the sub microgrid, resulting in a significant fluctuation in the power of the AC/DC hybrid microgrid groups and even leading to system disconnection in severe cases. Therefore, it is necessary to design a secondary control strategy for ILC based on primary control.

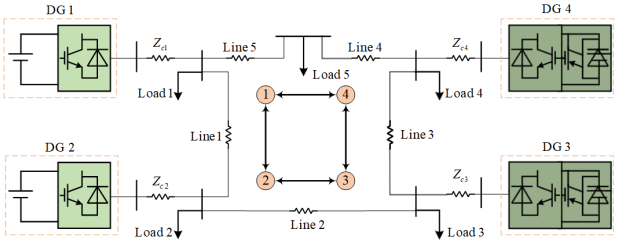

Fig. 2. Simulation model of AC subnet control strategy

The second consideration of the control objective Eq. (7) is to make the difference of the power mapping factors of the two-sided subnet at each ILC consistent and finally, converge to 0, which is formulated as

$$\lim_{t\to\infty} f_1(t) = \cdots = \lim_{t\to\infty} f_g(t) = \cdots = \lim_{t\to\infty} f_G(t) = 0 \tag{24}$$

$f_g(t)$ is designed as a constant state variable, and the cost quadratic control item ζ_g of ILC based on the consistency principle is formulated as

$$\begin{cases} \zeta_g = \Delta f_g \left(k_p^{Con} + \frac{k_i^{Con}}{s} \right) \\ \Delta f_g(t) = \sum_{h\in O} a_{gh} \left[f_g(t) - f_h(t) \right] \end{cases} \tag{25}$$

where $\Delta f_g(t)$ is the state difference between ILCg and adjacent ILCs at time t, and O is ILC set. k_p^{Con} and k_i^{Con} are the proportional and integral parameters of the PI controller, respectively.

So, according to (20) and (25), $\Delta f_g(t)$ can be formulated as

$$\Delta f_g(t) = \sum_{h\in O} a_{gh} \left\{ \left[\overline{\lambda_n^{dc}}(t) + \overline{\lambda_q^{dc}}(t) \right] - \left[\overline{\lambda_m^{ac}}(t) + \overline{\lambda_p^{ac}}(t) \right] \right\} \tag{26}$$

where subscripts p and q correspond to AC subnet and DC subnet connected to ILCh, respectively.

Based on the local control of ILC, the operation information of other ILCs is introduced, which is more conducive to the economic distribution of active power among all sub microgrids. Therefore, the control strategy of combining ILC primary control and secondary control is formulated as

$$P^*_{ILC,g} = f_g\left(k_p^{\mathrm{ILC}} + \frac{k_i^{\mathrm{ILC}}}{s}\right) - \gamma_g^{\omega} + \eta_g^{U} + \zeta_g \qquad (27)$$

4. Example analysis

4.1. Verification of AC subnet control strategy

To verify the effectiveness of the flow sub microgrid control strategy submitted in this paper, an AC microgrid simulation model, as shown in Fig. 2, is built based on MATLAB/Simulink. The AC subnet consists of four DG1, DG2, DG3, and DG4 with a rated voltage of 380 V. The power mapping factor of each DG unit is expressed as $\lambda(P_i) = 2\alpha_i P_i + \beta_i$. The values of control parameters and system parameters are shown in Table 1. Each DG is equipped with a corresponding load. The active load adopts resistive load, and the reactive load adopts inductive load.

The initial active load of the AC subnet is 480 kW, and the reactive load is 60kVA. After 2 s, increase the active load of Load 5 by 60 kW and the reactive load by 10kVA. After 3 s, reduce the active load of Load1 by 60 kW and the reactive load by 10kVA. After 4.5 s, Load5 returns to the starting load. The simulation results of the AC subnet under different control strategies are shown in Fig. 3. In addition, the DG unit using only ordinary droop control strategy and ordinary droop combined with classical consistency protocol strategy are compared as a control example.

From Fig. 3(a) to Fig. 3(d), the traditional droop control strategy leads to slow convergence speed and large allocation error, and the frequency cannot be restored to the reference value all the time. After introducing the secondary control based on consistency, the power allocation effect between DGs is improved, and the power mapping factor can converge uniformly.

From Fig. 3(e) to Fig. 3(h), the traditional droop control strategy realizes the proportional distribution of reactive power among DGs due to the inconsistent voltage of each DG node. The secondary control based on consistency can realize the distribution principle of reactive power. In addition, each DG node can be restored soon to the reference value.

4.2. Verification of DC subnet control strategy

To verify the effectiveness of the DC subnet control strategy, the system model shown in Fig. 4 is taken as the research object for simulation analysis. The DC subnet consists of three DG1, DG2, and DG3 with a rated voltage of 380 V. The values of control parameters and system parameters are shown in Table 2. The initial active load is set to 350 kW. After 1.5 s, increase the active load to 700 kW. The simulation results of the DC subnet under different control strategies are shown in Fig. 5.

From Fig. 5(a) to Fig. 5(d), the voltage of each DG node is inconsistent, resulting in that each DG unit cannot allocate active power in strict accordance with the equal incremental principle under the traditional control strategy. The control strategy proposed in this paper introduces the consistency algorithm based on the conventional droop control strategy, which overcomes the inherent defects of the conventional droop, realizes the accurate distribution of active power, and restores the node voltage to the reference value.

4.3. Verification of intergroup control strategy for AC/DC hybrid microgrid

To verify the effectiveness of the intergroup control strategy of the DC hybrid microgrid submitted in this paper, an AC/DC hybrid microgrid groups simulation model, as shown in Fig. 6, is built based on MATLAB/Simulink. The AC/DC hybrid microgrid groups comprises two AC sub microgrids MG1 and MG2, with a rated voltage of 380 V, and two DC sub microgrids MG3 and MG4, with a rated voltage of 700 V, including five AC DG units and five DC DG units. The values of α and β are shown in Table 3. The public bus of each subnet is equipped with a corresponding load. The active load adopts resistive load, and the reactive load adopts inductive load. Each subnet contains two DG units that can communicate with ILCs, and the interlinking converter ILC2 can communicate with the other two ILCs in two directions. Load, line parameters, and system control parameters are shown in Table 4.

In $0 \sim 2.5$ s, ILC is placed in the locked state, and each subnet reaches the stable operation state by itself. At 2.5 s, the ILC is placed in the open state, and the whole microgrid groups can realize the economic distribution of power through the transmission of active power between microgrids. At 5.5 s, increase the active load of the DC sub microgrid from 100 kW to 210 kW. The operation simulation results of the AC/DC hybrid microgrid groups are shown in Fig. 7.

As shown from Fig. 7(a) to Fig. 7(b), each DG node can converge quickly and uniformly under the internal control strategy of the subnet. After the ILC is put into use at 2.5s, each ILC quickly adjusts the exchange power between the subnets to reach a consistency on the power mapping factor of each subnet. During this period, the economic distribution within each subnet can still be maintained. In the subsequent process of load increase, the AC/DC hybrid microgrid groups control strategy can still meet the target requirements.

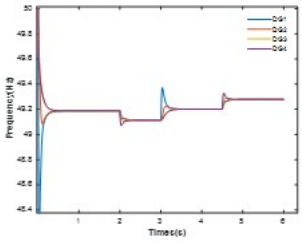

(a)Node frequency under traditional droop control strategy

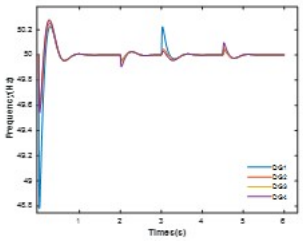

(b)Node frequency under three-level control based on consistency

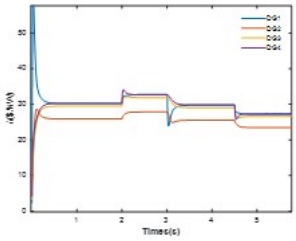

(c)Power mapping factor under traditional droop control strategy

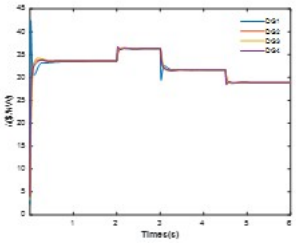

(d)Power mapping factor under three-level control based on consistency

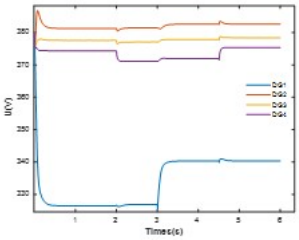

(e)Node voltage under traditional droop control strategy

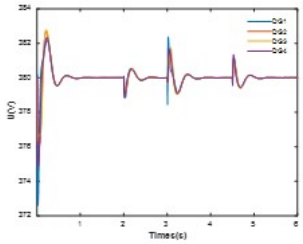

(f)Node voltage under three-level control based on consistency

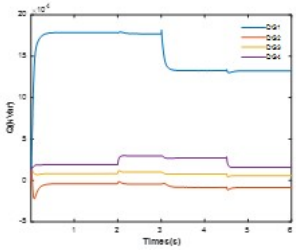

(g)Reactive power distribution under traditional droop control strategy

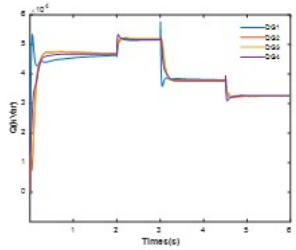

(h)Reactive power distribution under three-level control based on consistency

Fig. 3. Simulation results of AC subnet under different control strategies.

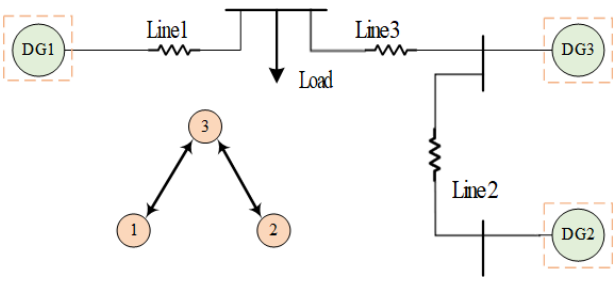

Fig. 4. Simulation model of DC subnet control strategy

As shown from Fig. 7(c) to Fig. 7(d), under the action of the internal control strategy and ILC control strategy of the microgrid, the frequency of the AC subnet and the voltage of the DC subnet can be quickly restored to the reference value to ensure the power balance of the microgrid groups.

As shown from Fig. 7(e) to Fig. 7(f), the DG nodes in each subnet distribute reactive power according to the principle of equal proportion distribution. When the DC load changes, the system stability is realized by exchanging energy under the action of inter-group control strategy. Under the action of secondary voltage adjustment, the voltage of

Table 1. Control strategy and system parameters of AC subnet

Control parameters	Reference value	System parameter	Reference value
α_1, β_1	0.08/2.25	Line /Ω	0.12 + j0.1
α_2, β_2	0.062/4.20	Line 2/Ω	0.175 + j0.58
α_3, β_3	0.075/3.25	Line3 /Ω	0.12 + j0.1
α_4, β_4	0.070/4.05	Line 4/Ω	0.12 + j0.1
k_{ac}^{P}	0.01	Line 5/Ω	0.175 + j0.58
k_{ac}^{Q}	0.001	Z_c/Ω	0.03 + j0.65
c_{agg}	0.2	Load 1(kV · A)	300 + j20
$k_p^{ac,,2}/k_i^{ac,,}$	0.75/1	Load2,Load 5(kV · A)	40 + j10
$k_p^{\omega}/k_i^{\omega}$	0.5/20	Load3,Load 4(kV · A)	50 + j10
k_p^{Q}/k_i^{Q}	0.001/1	$k_p^{ac,U}/k_i^{ac,U}$	0.1/20

Table 2. Control strategy and system parameters of DC subnet

Control and System parameters	Reference Value	Control and System parameters	Reference Value
α_1, β_1	0.062/4.2	Line 1/Ω	0.23
α_2, β_2	0.08/2.25	Line 2/Ω	0.12
α_3, β_3	0.072/3.6	Line3/ Ω	0.18
k_{dc}^{P}	0.01	Load (kW)	350
d_{avg}	0.2	$k_p^{dc,U}/k_i^{dc,U}$	1/10
$k_p^{dc,\lambda}/k_i^{dc,\lambda}$	0.1/1		

each subnet can be restored to the reference value.

5. Conclusion

Aiming at the stability optimization problem of the AC/DC hybrid microgrid groups, a distributed optimization control strategy for the AC/DC hybrid microgrid groups is proposed in this paper. At the level of subnet control, this paper introduces the secondary control term based on consistency protocol into the improved power mapping factor droop control strategy, realizes the distributed optimal control of AC and DC subnet, realizes the proportional distribution of reactive power of AC subnet and the economic distribution of DC subnet, and can restore the frequency and voltage of subnet to the reference value. In terms of microgrid inter-group control, the ILC control strategy based on the deviation of the power mapping factor realizes the economic distribution of power between AC and DC sub microgrids. In conclusion, the simulation analysis shows that the control strategy proposed in this paper can achieve the established control objectives.

Acknowledgements

This work was supported in part by scientific and technological project (031900KK52210009, GDKJXM20212078) of China Southern Power Grid Corporation.

References

[1] G. Weiss, Q.-C. Zhong, T. C. Green, and J. Liang, (2004) *"H/sup/spl infin//repetitive control of DC-AC converters in microgrids"* **IEEE Transactions on Power Electronics *19***(1): 219–230. DOI: 10.1109/TPEL.2003.820561.

[2] J. P. Lopes, C. L. Moreira, and A. Madureira, (2006) *"Defining control strategies for microgrids islanded operation"* **IEEE Transactions on power systems *21***(2): 916–924. DOI: 10.1109/TPWRS.2006.873018.

[3] S. Zuo, A. Davoudi, Y. Song, and F. L. Lewis, (2016) *"Distributed finite-time voltage and frequency restoration in islanded AC microgrids"* **IEEE Transactions on Industrial Electronics *63***(10): 5988–5997. DOI: 10.1109/TIE.2016.2577542.

[4] Q. Cao and W. Xie, (2020) *"Optimal Frequency Control for Inverter-Based Micro-Grids Using Distributed Finite-Time Consensus Algorithms"* **IEEE Access *8***: 185243–185252. DOI: 10.1109/ACCESS.2020.3030026.

[5] A. Bidram and A. Davoudi, (2012) *"Hierarchical structure of microgrids control system"* **IEEE Transactions on Smart Grid *3***(4): 1963–1976. DOI: 10.1109/TSG.2012.2197425.

[6] J. M. Guerrero, J. C. Vasquez, J. Matas, L. G. De Vicuña, and M. Castilla, (2010) *"Hierarchical control of droop-controlled AC and DC microgrids—A general ap-*

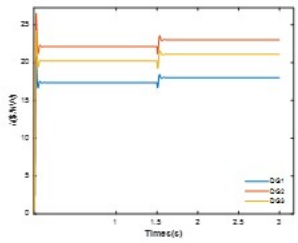

(a)Power mapping factor under traditional droop control strategy

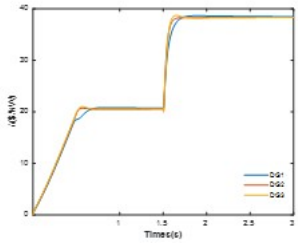

(b)Power mapping factor under three-level control based on consistency

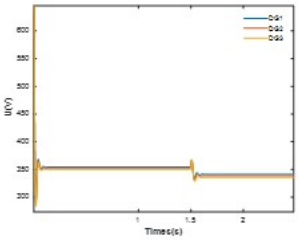

(c)Node voltage under traditional droop control strategy

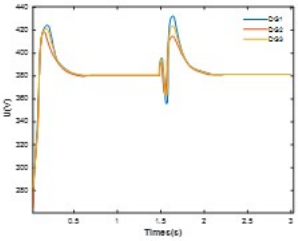

(d)Node voltage under three-level control based on consistency

Fig. 5. Simulation results of DC subnet under different control strategies.

Table 3. The cost factor of DGs

DG Unit	Reference Value	DG Unit	Reference Value
DG11	0.005/0.75	DG31	0.24/1.34
DG12	0.035/1.25	DG32	0.23/1.42
DG13	0.026/1.46	DG33	0.012/0.74
DG14	0.019/1.97	DG41	0.24/1.34
DG21	0.004/0.82	DG42	0.23/1.42
DG22	0.032/1.28	DG43	0.012/0.74

Table 4. Line parameters and initial load

Parameter	Values	Parameter	Values
Line 11/Ω	$0.26+\mathrm{j}0.21$	k_{ac}^{P}	0.01
Line 12/Ω	$0.11+\mathrm{j}0.14$	k_{ac}^{Q}	0.003
Line 13/Ω	$0.13+\mathrm{j}0.13$	k_p^{Con}/k_i^{Con}	0.0075/0.1
Line 14/Ω	$0.16+\mathrm{j}0.18$	k_p^{ILC}/k_i^{ILC}	0.005/0.2
Line 21/Ω	$0.26+\mathrm{j}0.21$	$k_p^{ac,\lambda}/k_i^{ac,\lambda}$	0.75/1
Line 22/Ω	$0.11+\mathrm{j}0.14$	$k_p^{\omega}/k_i^{\infty}$	0.5/20
Line 31/Ω	0.18	k_p^{Q}/k_i^{Q}	0.001/1
Line 32/Ω	0.24	$k_p^{ac,U}/k_i^{ac,U}$	0.1/20
Line 33/Ω	0.16	$k_p^{dc,U}/k_i^{dc,U}$	1/10
Line 41/Ω	0.18	k_{dc}^{P}	0.01
Line 42/Ω	0.24	k_p/k_i	0.001/0.2
Line 43/Ω	0.16	$k_p^{dc,\lambda}/k_i^{dc,\lambda}$	0.1/1
Line 1/Ω	$0.12+\mathrm{j}0.13$	Line 2/Ω	$0.12+\mathrm{j}0.13$
Line 3/Ω	0.8	Line 4/Ω	0.8
Load 1/(kV · A)	$80+\mathrm{j}30$	Load2 /(kV · A)	$70+\mathrm{j}20$
Load3 /(kV · A)	70	Load 4/(kV · A)	100

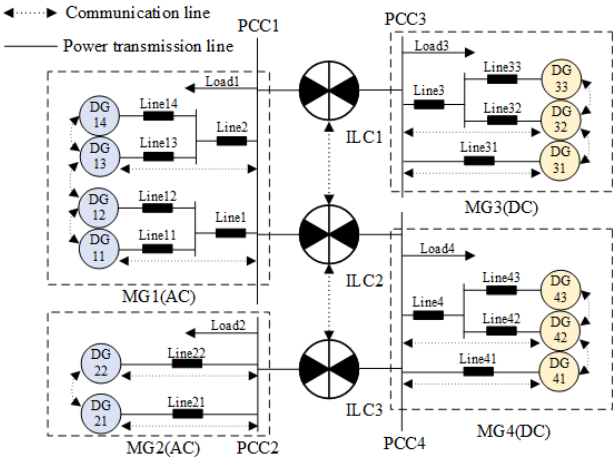

Fig. 6. Simulation model of AC/DC hybrid microgrid groups system

proach toward standardization" **IEEE Transactions on industrial electronics** ***58***(1): 158–172. DOI: 10.1109/TIE.2010.2066534.

[7] J. W. Simpson-Porco, F. Dörfler, and F. Bullo, (2013) *"Synchronization and power sharing for droop-controlled inverters in islanded microgrids"* **Automatica** ***49***(9): 2603–2611.

[8] Y. Xu and H. Sun, (2017) *"Distributed finite-time convergence control of an islanded low-voltage AC microgrid"* **IEEE Transactions on Power Systems** ***33***(3): 2339–2348. DOI: doi={10.1109/TPWRS.2017.2743011}.

[9] M. Shi, X. Chen, J. Zhou, Y. Chen, J. Wen, and H. He, (2019) *"PI-consensus based distributed control of AC microgrids"* **IEEE Transactions on Power Systems** ***35***(3): 2268–2278. DOI: 10.1109/TPWRS.2019.2950629.

[10] A. Shyam, S. Anand, and S. R. Sahoo, (2020) *"Effect of communication delay on consensus-based secondary controllers in DC microgrid"* **IEEE Transactions on Industrial Electronics** ***68***(4): 3202–3212. DOI: 10.1109/TIE.2020.2978719.

[11] Z. Wang, W. Wu, and B. Zhang, (2015) *"A fully distributed power dispatch method for fast frequency recovery and minimal generation cost in autonomous microgrids"* **IEEE Transactions on Smart Grid** ***7***(1): 19–31. DOI: 10.1109/TSG.2015.2493638.

[12] M. A. Shahab, B. Mozafari, S. Soleymani, N. M. Dehkordi, H. M. Shourkaei, and J. M. Guerrero, (2019) *"Stochastic Consensus-Based Control of muGs With Communication Delays and Noises"* **IEEE Transactions on Power Systems** ***34***(5): 3573–3581. DOI: 10.1109/TPWRS.2019.2905433.

[13] Q. Li, D. W. Gao, H. Zhang, Z. Wu, and F.-Y. Wang, (2017) *"Consensus-based distributed economic dispatch control method in power systems"* **IEEE transactions on smart grid** ***10***(1): 941–954. DOI: 10.1109/TSG.2017.2756041.

[14] X. Shen, H. Wang, D. Zhang, J. Li, R. Wang, and Q. Su, (2020) *"Distributed finite-time secondary voltage restoration of droop-controlled islanded microgrids"* **IEEE Access** ***8***: 118183–118191. DOI: 10.1109/ACCESS.2020.3004340.

[15] M. A. Shahab, B. Mozafari, S. Soleymani, N. M. Dehkordi, H. M. Shourkaei, and J. M. Guerrero, (2019) *"Distributed consensus-based fault tolerant control of islanded microgrids"* **IEEE Transactions on Smart Grid** ***11***(1): 37–47. DOI: 10.1109/TSG.2019.2916727.

[16] H. Yu, S. Niu, Z. Shao, and L. Jian, (2022) *"A scalable and reconfigurable hybrid AC/DC microgrid clustering architecture with decentralized control for coordinated operation"* **International Journal of Electrical Power & Energy Systems** ***135***: 107476.

[17] Y. Zheng, S. Niu, Y. Shang, Z. Shao, and L. Jian, (2019) *"Integrating plug-in electric vehicles into power grids: A comprehensive review on power interaction mode, scheduling methodology and mathematical foundation"* **Renewable and Sustainable Energy Reviews** ***112***: 424–439.

[18] H. Yu, S. Niu, Y. Zhang, and L. Jian, (2020) *"An integrated and reconfigurable hybrid AC/DC microgrid architecture with autonomous power flow control for nearly/net zero energy buildings"* **Applied Energy** ***263***: 114610.

[19] Y. Zheng, Z. Shao, and L. Jian, (2021) *"The peak load shaving assessment of developing a user-oriented vehicle-to-grid scheme with multiple operation modes: The case study of Shenzhen, China"* **Sustainable Cities and Society** ***67***: 102744.

[20] F. Dörfler, J. W. Simpson-Porco, and F. Bullo, (2015) *"Breaking the hierarchy: Distributed control and economic optimality in microgrids"* **IEEE Transactions on Control of Network Systems** ***3***(3): 241–253.

[21] H.-J. Yoo, T.-T. Nguyen, and H.-M. Kim, (2019) *"Consensus-based distributed coordination control of hybrid AC/DC microgrids"* **IEEE Transactions on Sustainable Energy** ***11***(2): 629–639.

[22] P. Lin, C. Jin, J. Xiao, X. Li, D. Shi, Y. Tang, and P. Wang, (2018) *"A distributed control architecture for global system economic operation in autonomous hybrid AC/DC microgrids"* **IEEE Transactions on Smart Grid** ***10***(3): 2603–2617. DOI: 10.1109/TSG.2018.2805839.

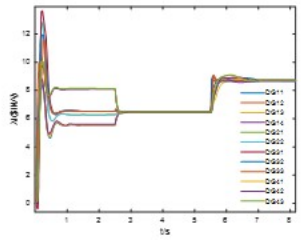

(a)Power mapping factor of each DG node

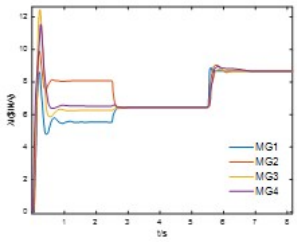

(b)Average power mapping factor of each subnet

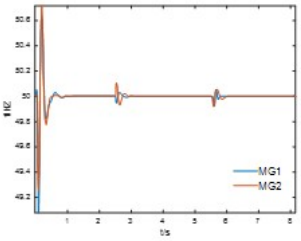

(c)Node voltage under traditional

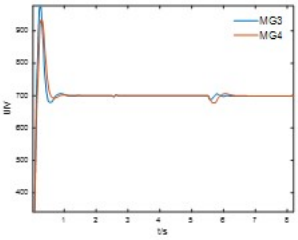

(d)Node voltage under three-level

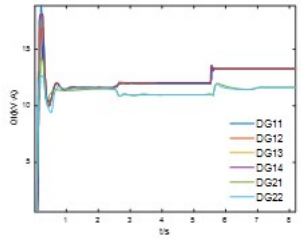

(e)Reactive power distribution of AC DG node

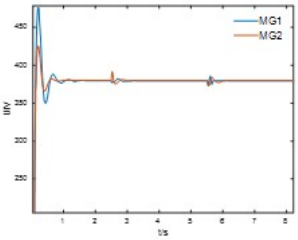

(f)Voltage fluctuation of AC subnet

Fig. 7. Simulation results of the AC/DC hybrid microgrid groups control strategy.

[23] J. Zhou, H. Zhang, Q. Sun, D. Ma, and B. Huang, (2017) *"Event-based distributed active power sharing control for interconnected AC and DC microgrids"* **IEEE Transactions on Smart Grid** *9*(6): 6815–6828. DOI: doi={10.1109/TSG.2017.2724062}.

[24] J. Yang, J. Hou, Y. Liu, and H. Zhang, (2021) *"Distributed cooperative control method and application in power system"* **Trans. China Electrotech. Soc** *36*: 4035–4049.